SUPPLEMENTAL MATERIAL

Supplemental Methods:

Reagents, Pharmacologic Inhibitors and Antibodies

Recombinant NAMPT protein (CY-E1251) was obtained from MBL Lifescience. The NAMPT specific inhibitor (FK866, Cat.# F8557) and monoclonal anti-β-actin−peroxidase antibody (cat.# A3854) were from Sigma. Rabbit anti-NAMPT(cat.# A300-372A), STIM2 (cat.# 4917S), anti-ORAI2 (cat.# ab180146) and PCNA (cat.#SC-7907) antibodies were purchased from Bethyl Laboratories, Inc, Cell Signaling, ABCAM, Santa Cruz, respectively. NAD/NADH Quantitation Colorimetric Kit (cat.# K337-100) was from BioVision, Inc. Cell death assays were performed using a cytotoxicity detection Kit (LDH, cat.# 11644793001, Sigma) and cell viability was examined using CellTiter 96 Aqueous One Solution Cell Proliferation Assay kit (Cat.# G3580, Promega). Cell migration was conducted using Falcon™ Cell Culture Inserts (Fisher, Cat.# 08-771-12) and migrated cells were stained by 1% aqueous Crystal Violet solution (Electron Microscopy Sciences, Cat.# RT 26088-10). H_2O_2 (100μM, Sigma, Cat.# ab66110) was used as an apoptosis stimulus for hPASMCs. Cell apoptosis was examined using an in situ BrdU –Red DNA fragmentation (TUNEL) kit. Verapamil hydrochloride (Sigma, Cat# V4629-1G), a phenylalkylamine Ca^{2+} channel blocker, was used to study the effect of L-type Calcium channel on the SOCE in hPASMCs.

Human PASMCs

Human PASMCs from control and PAH patients were obtained and isolated as previously described.[1]

Supplemental Tables:

Supplemental Table 1- Clinical Characteristics of Control and PAH Subjects

Characteristic	Control	PAH
n	53	103
Age (years)*	55 ± 9	55 ± 14
Female gender (n)	42	82
Race (n)		
White	42	80
Black	11	23
PAH Classification (%)		
Idiopathic	42	
Heritable	2	
Associated with CTD	56	
Mean PA pressure (mmHg)*		42 ± 17
PAOP (mmHg)*		10 ±3
Cardiac Output (l/min)*		4.5 ± 1.3
6 minute walk distance (m)*		332 ± 163

* plus or minus standard deviation

CTD: connective tissue disease

PAOP: pulmonary artery occlusion pressure

Supplemental Figures and Figure Legends:

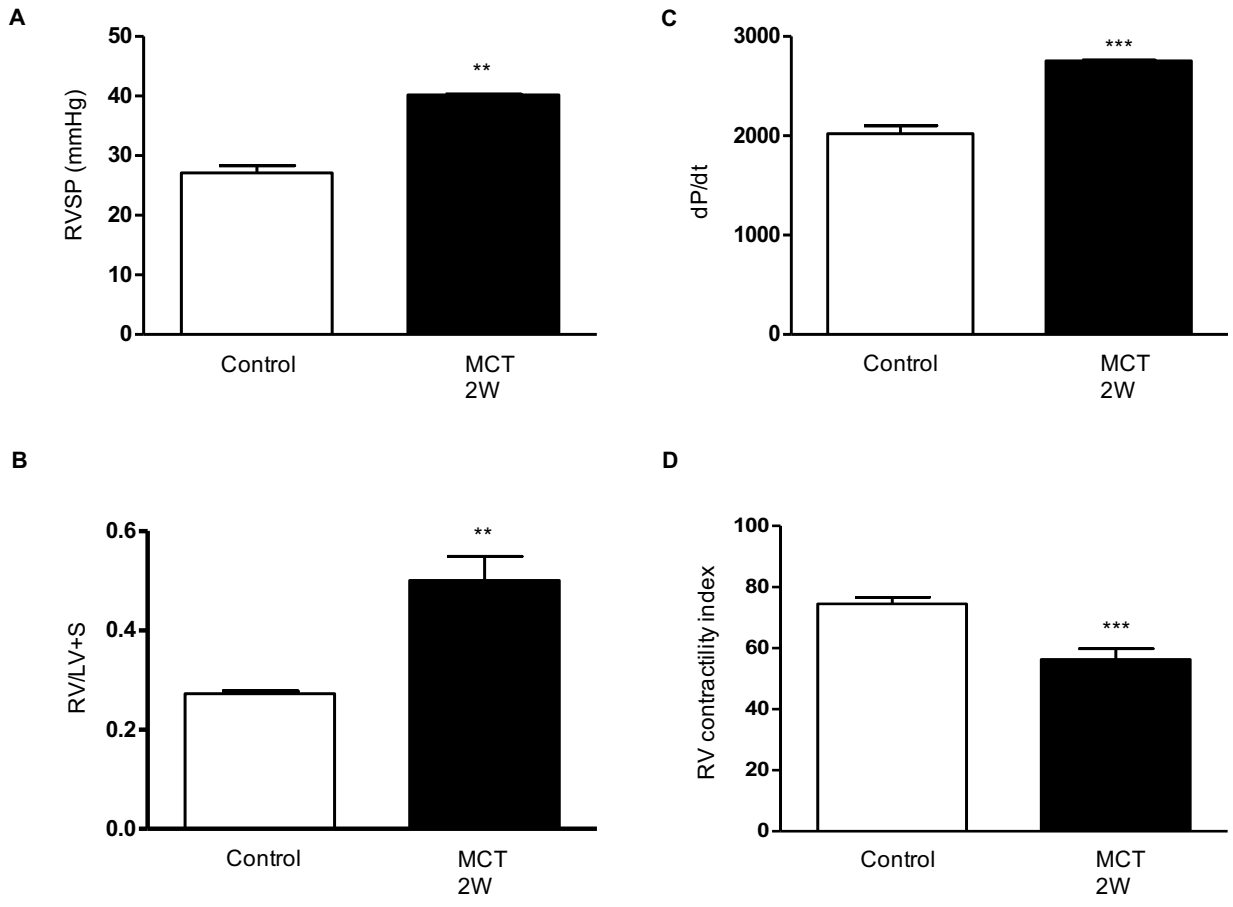

Figure S1: Phenotypic characterization of a rat model of monocrotaline (MCT)-mediated pulmonary hypertension at 2-week time point after MCT injection compared to controls. A) RVSP data quantification; B) RV/(LV+S) data; C) maximum dP/dt data quantification; D) RV contractility index data. The RV contractility index was calculated as $(dp/dt)_{max}$/instantaneous RV $pressure_{max,}$ as demonstrated previously.[2] Results are expressed as mean ± SEM; n = 10 per group. **, $p < 0.01$; ***, $p < 0.001$.

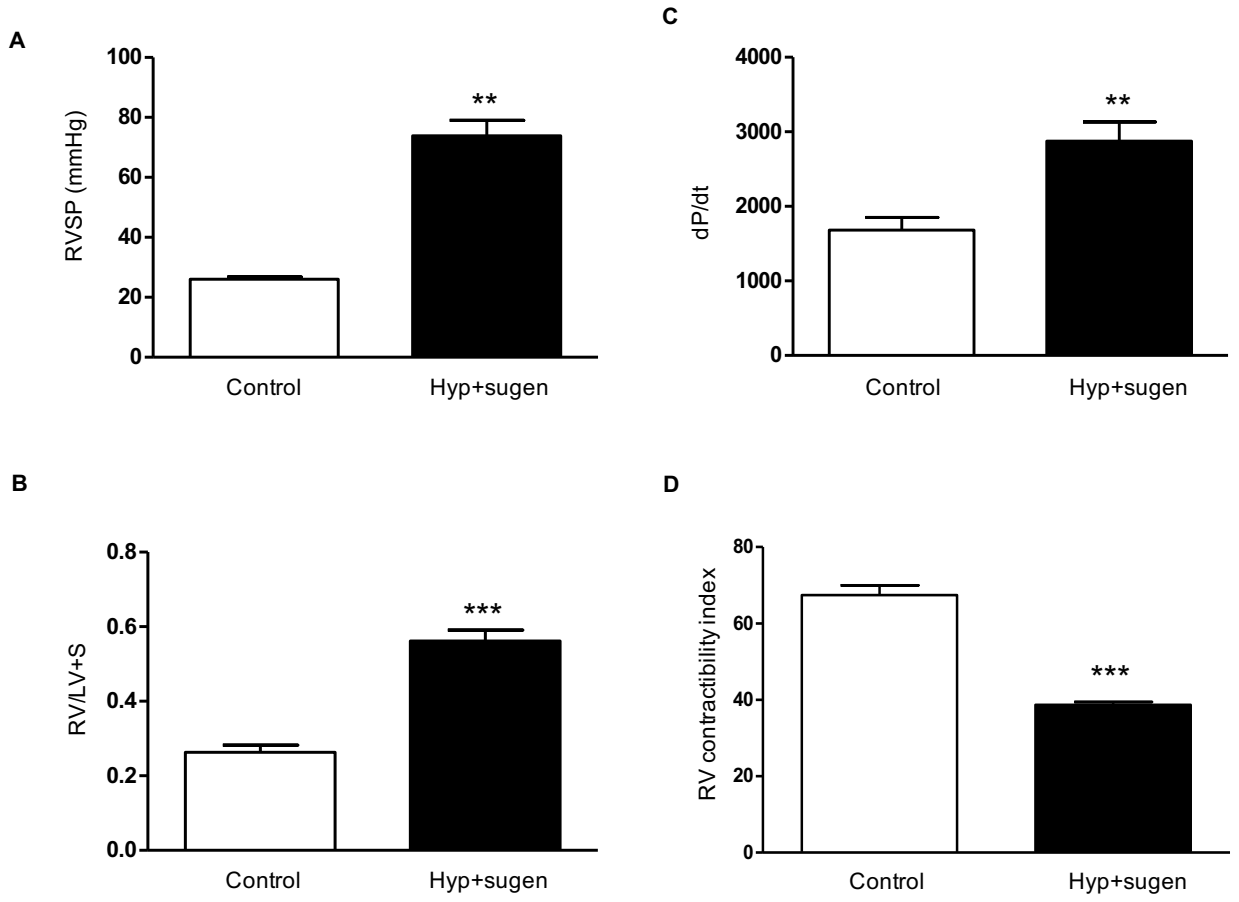

Figure S2: Phenotypic characterization of a rat model of pulmonary hypertension-mediated by hypoxia plus sugen after three-week hypoxia and two-week reoxygenation. A) RVSP data quantification; B) RV/(LV+S) data; C) maximum dP/dt data quantification; D) RV contractility index data. The RV contractility index was calculated as $(dp/dt)_{max}$ /instantaneous RV $pressure_{max,}$ as demonstrated previously.[2] Results are expressed as mean ± SEM; n = 6 per group. $p < 0.01$; ***, $p < 0.001$.

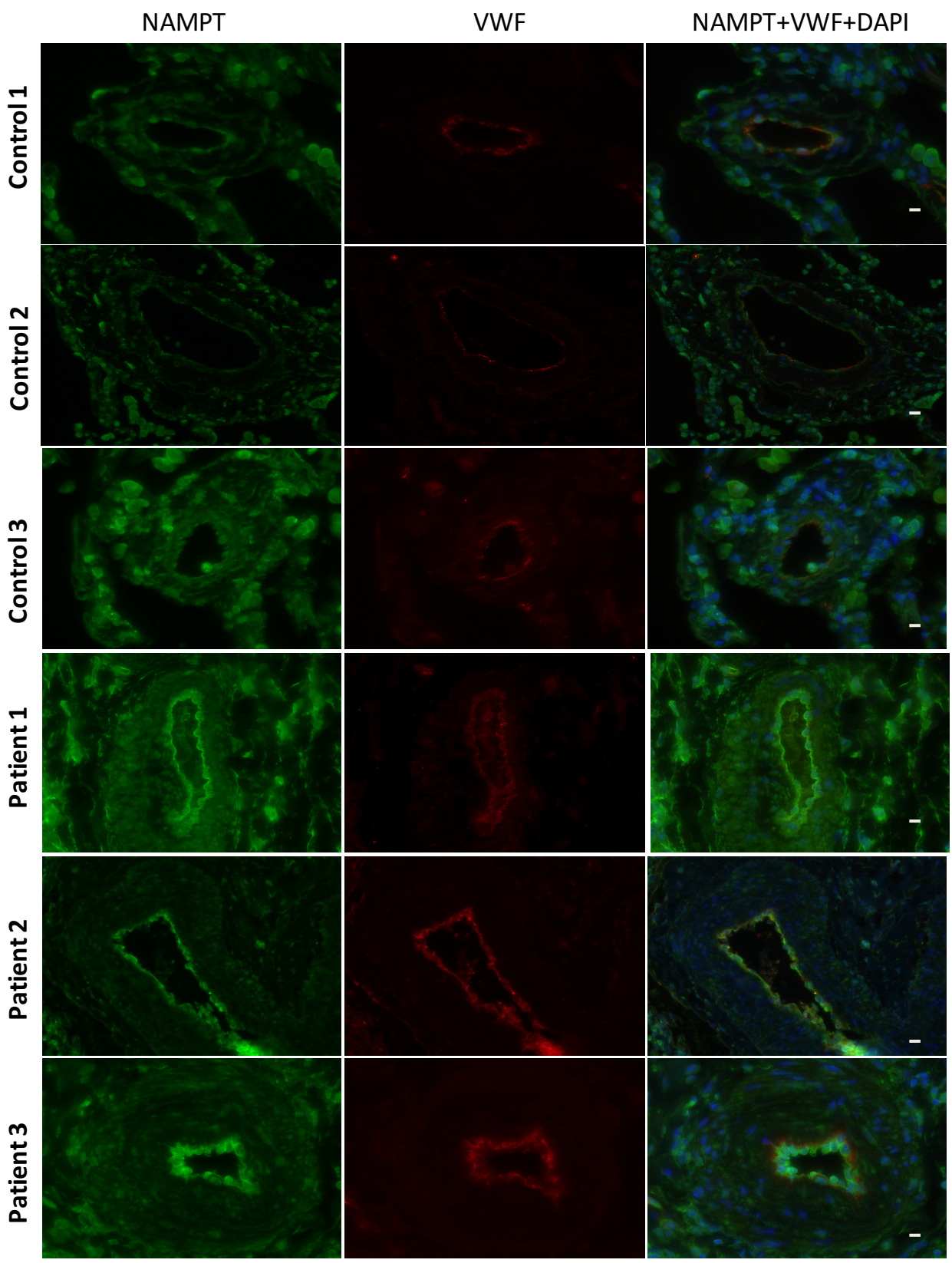
NAMPT
VWF
NAMPT+VWF+DAPI
Control 1
Control 2
Control 3
Patient 1
Patient 2
Patient 3

Figure S3. Lung immunofluorescence staining demonstrates increased NAMPT expression in pulmonary artery endothelial cells in patients with pulmonary arterial hypertension. Paraffin-embedded lung tissue sections were deparaffinized with xylene and rehydrated. Antigen retrieval was used before blocking in PBS with 10% normal goat serum, 0.1%BSA, 0.3% TX-100. The antigen retrieval solution is Tris-EDTA buffer (10 mM Tris Base, 1 mM EDTA solution, 0.05% Tween 20, pH 9.0). The dilutions for rabbit against NAMPT (Bethyl Laboratories, Inc. catalog# A300-372A) and Cy3-labelled mouse against smooth muscle actin are 1:100 and 1:300, respectively. Secondary antibody for NAMPT was Alexa Fluor® 488 Donkey anti-Rabbit IgG antibody (1:500). An anti-fade mounting media with DAPI (Life Science Inc) was used to fix the coverslip to a slide. The slides were examined using a Nikon Eclipse E800 fluorescence microscope, and the images were processed by MetaMorph software (Molecular Devices, Inc.). Size bar: 20 μm.

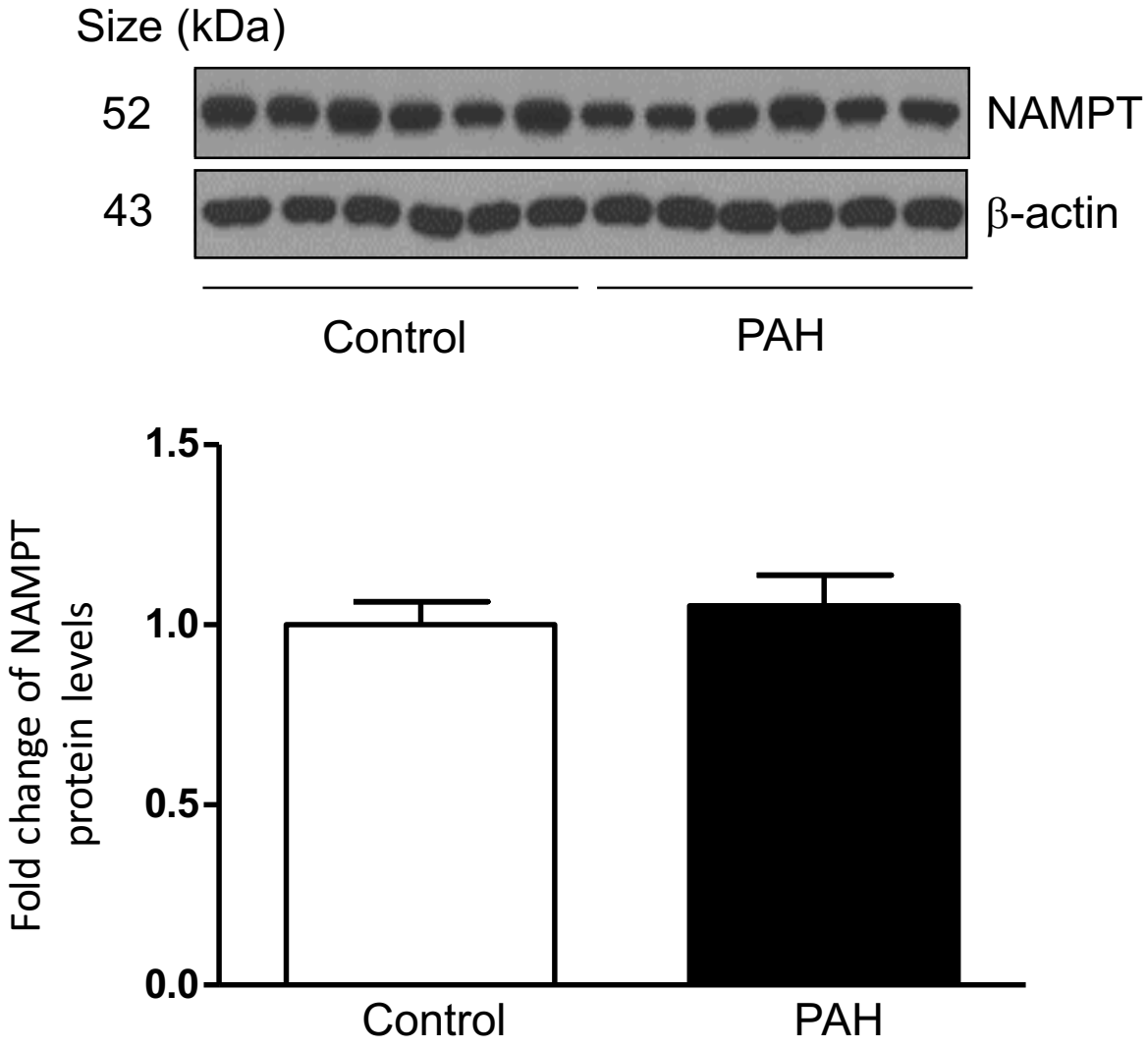

Figure S4. NAMPT expression in PASMCs from Controls and PAH patients. Representative Western blotting images and β-actin-normalized quantification of protein demonstrate that PASMC NAMPT expression is not significantly different in lungs from PAH patients when compared to non-PAH controls. N=6 each group. $p > 0.05$

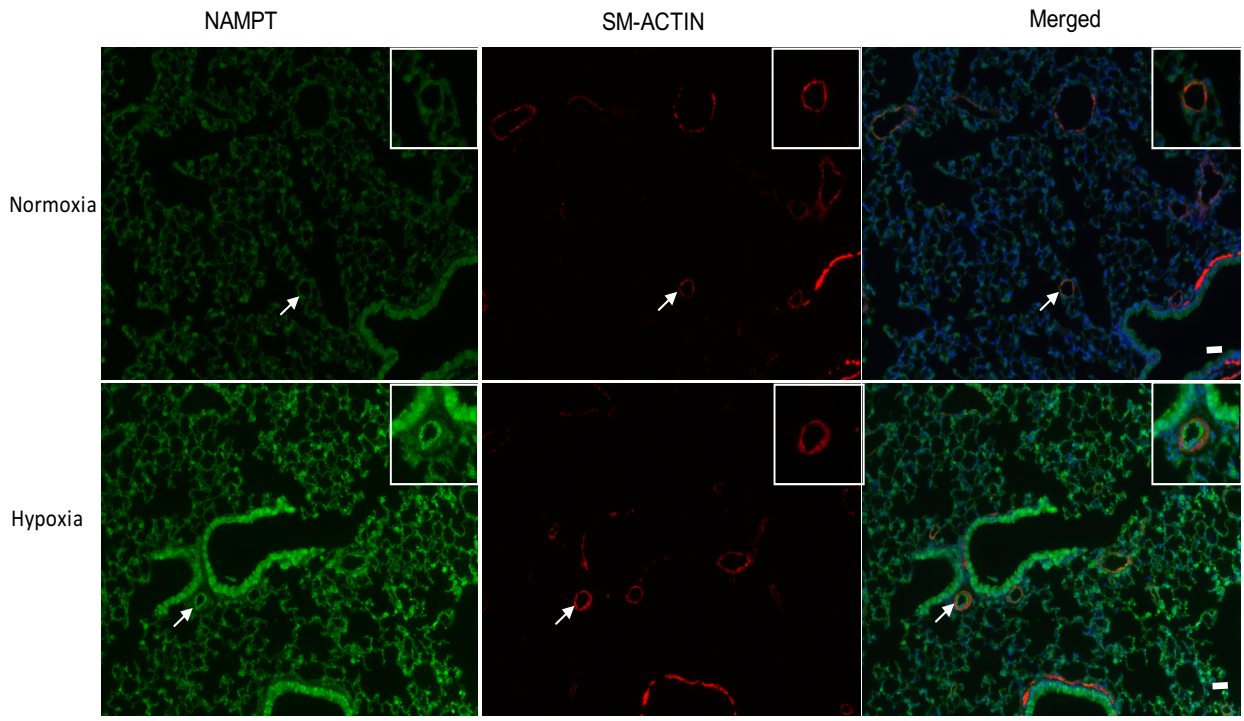

Figure S5. NAMPT expression in a mouse model of hypoxia induced PH. Immunofluorescence staining of lung tissues from mice after 4-week hypoxia exposure (10% O_2) when compared to normoxia demonstrate increased NAMPT expression in the pulmonary vasculature mainly in PAECs and the adventitia, but not in the media, as well as in alveolar and airway epithelial cells. A representative pulmonary vasculature pointed by an arrow was highlighted in the right corner of each image. Paraffin-embedded lung tissue sections were deparaffinized with xylene and rehydrated. Antigen retrieval was used before blocking in PBS with 10% normal goat serum, 0.1%BSA, 0.3% TX-100. The antigen retrieval solution is Tris-EDTA buffer (10 mM Tris Base, 1 mM EDTA solution, 0.05% Tween 20, pH 9.0). The dilutions for rabbit against NAMPT (Bethyl Laboratories, Inc. catalog# A300-372A) and Cy3-labelled mouse against smooth muscle actin are 1:100 and 1:300, respectively. Secondary antibody for NAMPT was Alexa Fluor® 488 Donkey anti-Rabbit IgG antibody (1:500). An anti-fade mounting media with DAPI (Life Science Inc) was used to fix the coverslip to a slide. The slides were examined using a Nikon Eclipse E800 fluorescence microscope, and the images were processed by MetaMorph software (Molecular Devices, Inc.). Size bar: 50 μm.

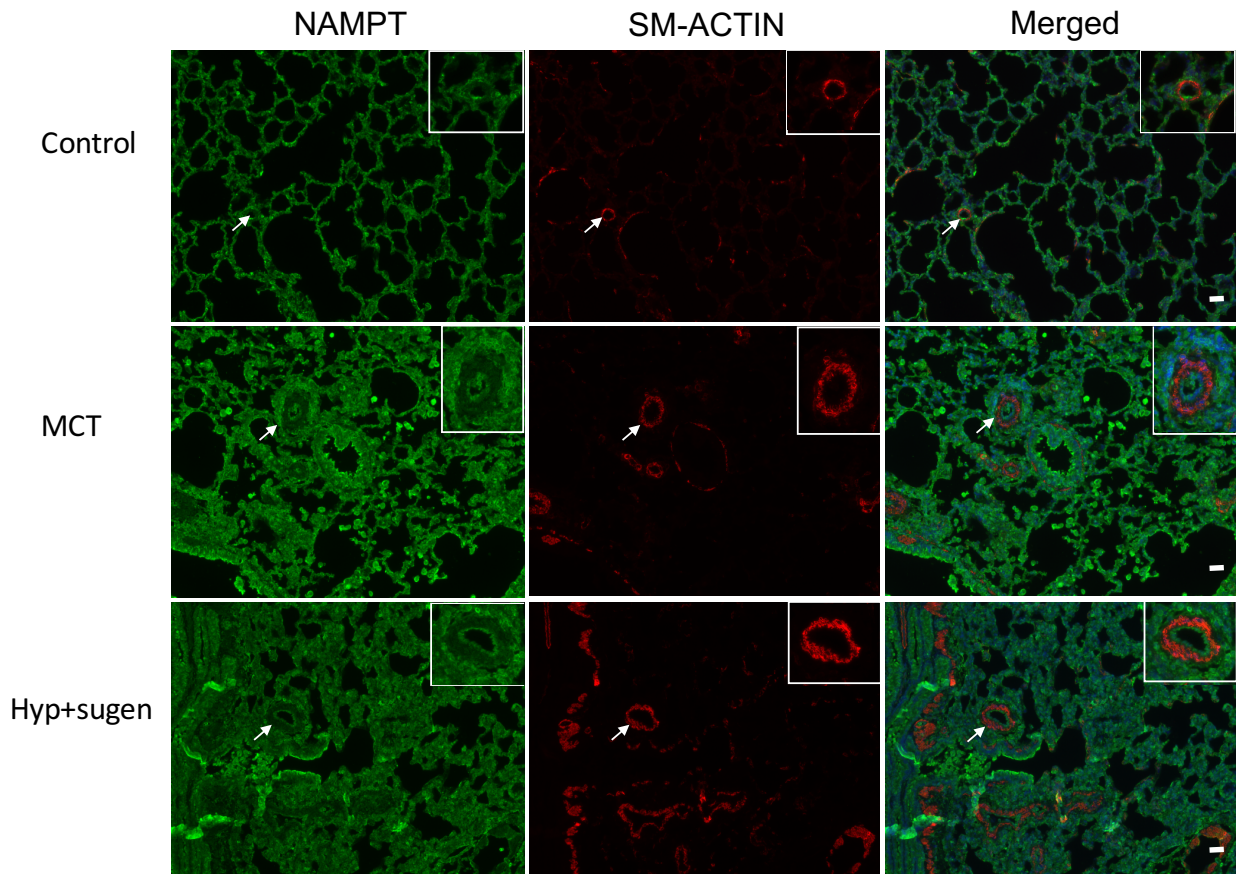

Figure S6. NAMPT expression in rat models of PH. Immunofluorescence staining of lung tissues from rats after monocrotaline treatment (2 weeks after monocrotaline injection) and rats after hypoxia+sugen treatment (3 weeks hypoxia exposure + 2 weeks reoxygenation) when compared to control healthy rats, demonstrate increased NAMPT expression in the pulmonary vasculature mainly in PAECs and the adventitia, but not in the media, as well as in alveolar macrophages, alveolar and airway epithelial cells. A representative pulmonary vasculature pointed by an arrow was highlighted in the right corner of each image. Paraffin-embedded lung tissue sections were deparaffinized with xylene and rehydrated. Antigen retrieval was used before blocking in PBS with 10% normal goat serum, 0.1%BSA, 0.3% TX-100. The antigen retrieval solution is Tris-EDTA buffer (10 mM Tris Base, 1 mM EDTA solution, 0.05% Tween 20, pH 9.0). The dilutions for rabbit against NAMPT (Bethyl Laboratories, Inc. catalog# A300-372A) and Cy3-labelled mouse against smooth muscle actin are 1:100 and 1:300, respectively. Secondary antibody for NAMPT was Alexa Fluor® 488 Donkey anti-Rabbit IgG antibody

(1:500). An anti-fade mounting media with DAPI (Life Science Inc) was used to fix the coverslip to a slide. The slides were examined using a Nikon Eclipse E800 fluorescence microscope, and the images were processed by MetaMorph software (Molecular Devices, Inc.). Size bar: 50 μm.

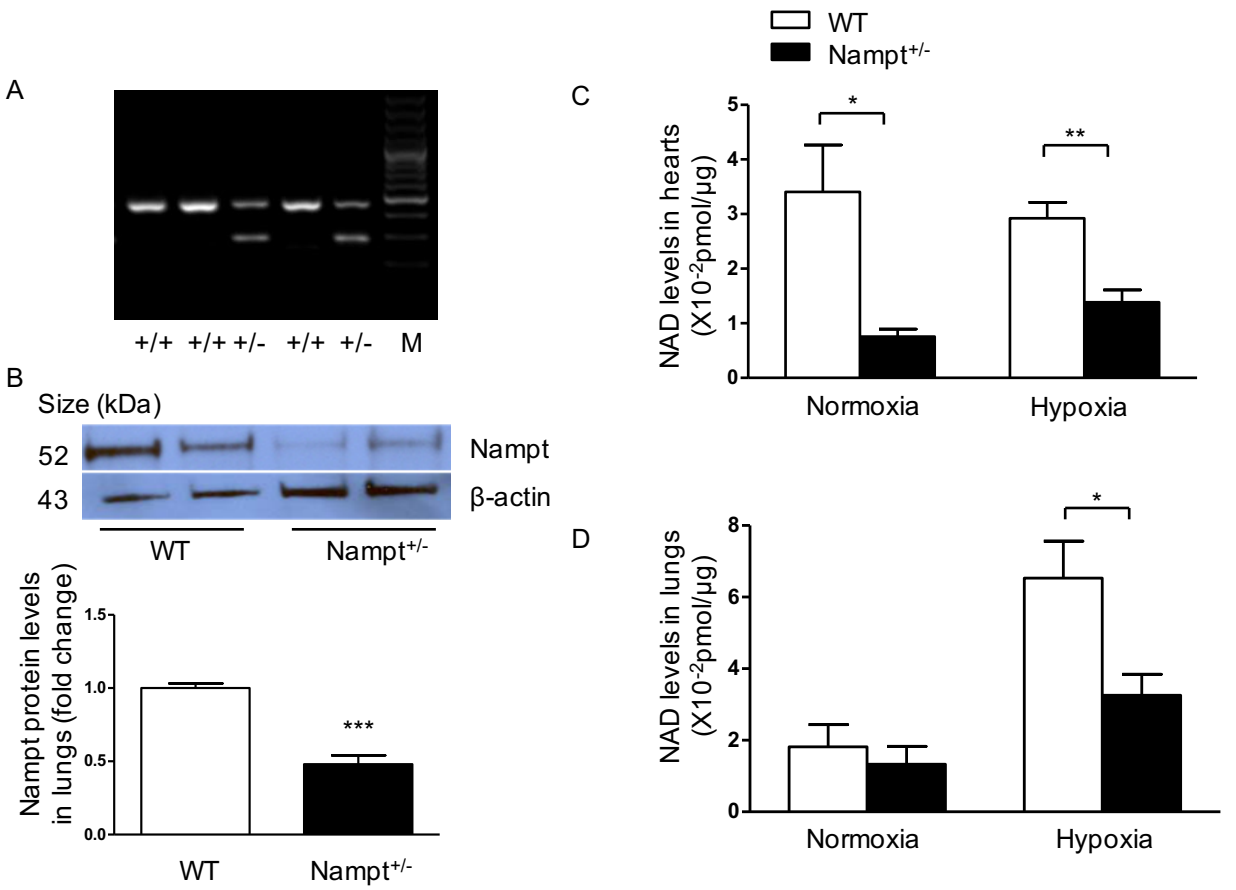

Figure S7. NAD levels in *Nampt*$^{+/-}$ mice. Compared to wild-type siblings, *Nampt*$^{+/-}$ mice exhibited significantly lower baseline levels of NAMPT in the lung tissue homogenates. NAD levels in the lung and heart tissues are significantly lower in *Nampt*$^{+/-}$ mice after 4-week hypoxia (10% O_2) exposure. A. Mouse genotyping data via PCR and agarose gel electrophoresis shows that the individuals with double bands (284 bp and 458 bp) are NAMPT heterozygous, with one band wild-type (458 bp). PCR primers: forward: 5'-CAGCAGCAGACCATTTTCAA - 3'; reverse primer: 5'-GGGAGTGACACAGCAAATCA-3'. B. Western blotting using lung homogenates shows *NAMPT*$^{+/-}$ mice exhibited significantly lower baseline levels of NAMPT in the lung tissue homogenates; C. NAD levels are significantly lower in the heart tissues from *Nampt*$^{+/-}$ mice under normoxia or hypoxia conditions; D. NAD levels are significantly lower in the lung tissues from *Nampt*$^{+/-}$ mice under hypoxia exposure. At baseline, NAD levels have a non-significant trend to be lower in the lung tissues from *Nampt*$^{+/-}$ mice. *, $P < 0.05$; **, $p < 0.01$; ***, $p<0.001$.

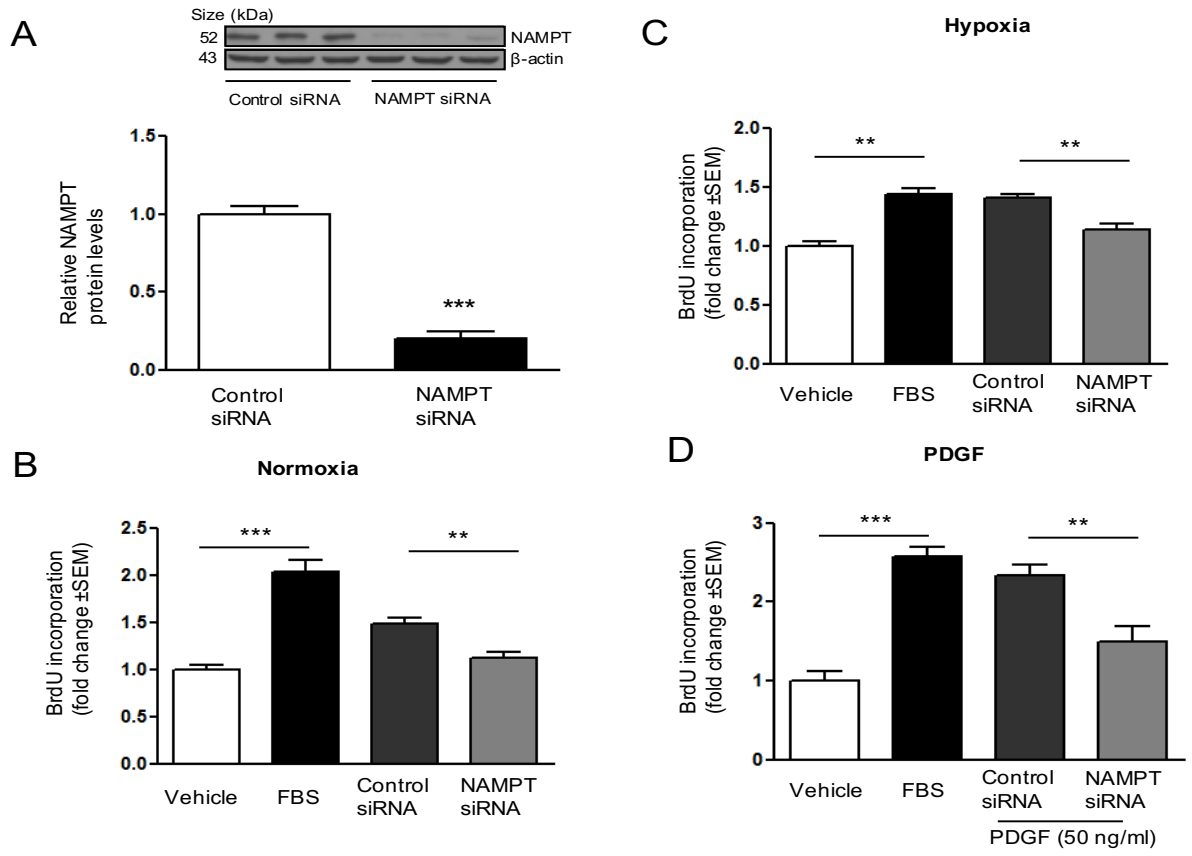

Figure S8. NAMPT downregulation via siRNA attenuates hPAMSC proliferation under normoxia, hypoxia or PDGF stimulation. PDGF = platelet-derived growth factor. A) A representative Western blotting image demonstrates that approximately 80% of NAMPT was silenced in hPASMCs ($p = 0.0003$). Using Lipofectamine™ RNAiMAX Reagent (Invitrogen, cat.# 13778-150), hPASMCs were transfected with NAMPT siRNA (L-000458-00) or scrambled siRNA (D-001810-02), which were purchased from Dharmacon (Thermo Fisher Scientific, Lafayette, CO, USA) according to the manufacturer's protocol. β-actin was used for normalization. Experiments were repeated more than three times. B-D. BrdU incorporation assays demonstrated that Silencing NAMPT via its specific siRNA attenuated hPAMSC proliferation under normoxia, hypoxia or PDGF stimulation. Results are expressed as mean ± SEM; n = 6 per group. $^{**}P < 0.01$; $^{***}P < 0.001$. FBS was used as a positive control for BrdU proliferation assays.

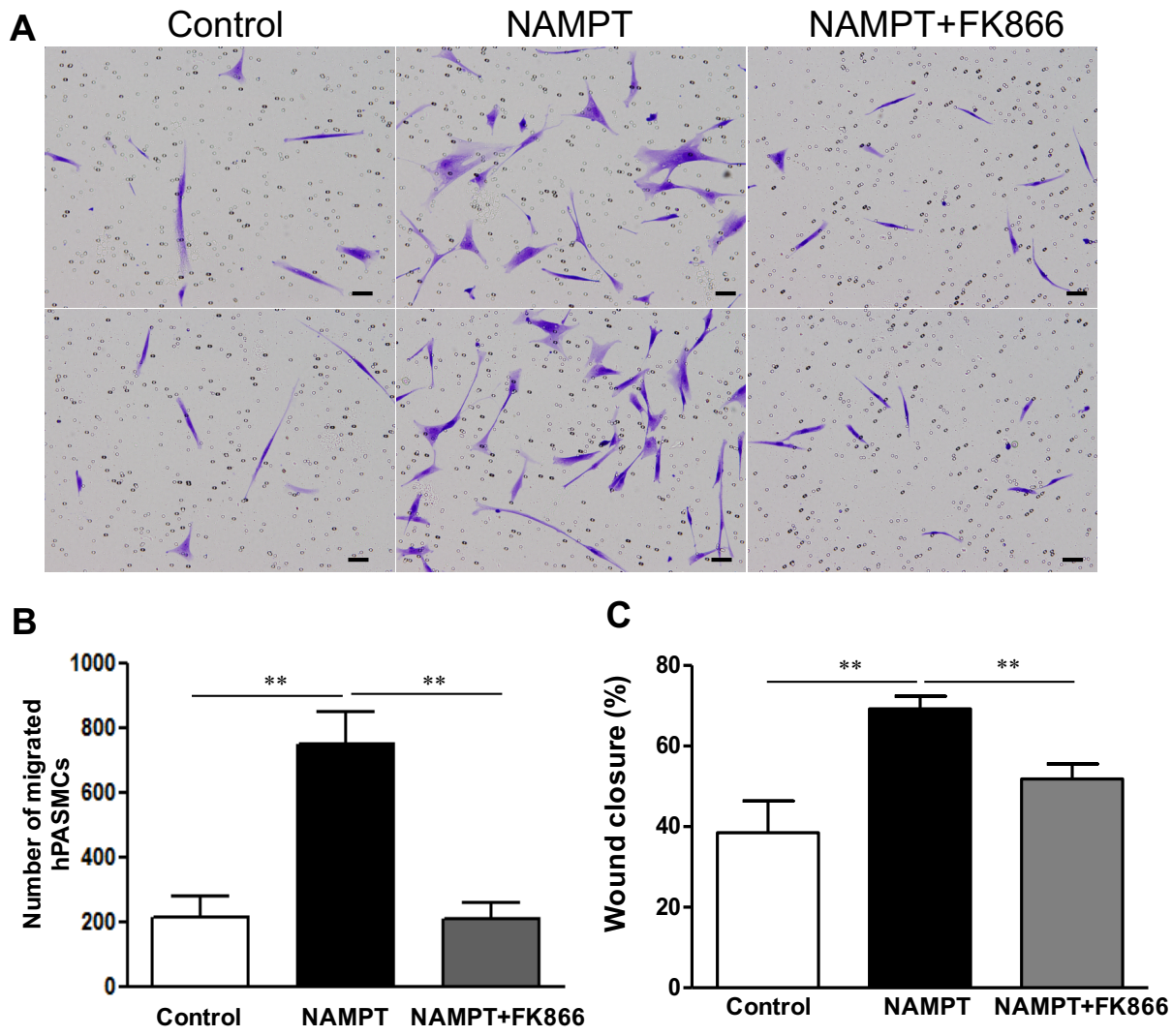

Figure S9. Transwell migration and wound healing assays demonstrate that recombinant NAMPT protein (rNAMPT) promotes hPASMC migration. A) Representative images and B) quantitative data from transwell migration assays (ANOVA $P < 0.05$). In brief, 50,000 cells were added into Falcon™ Cell Culture Inserts (Fisher, Cat.# 08-771-12) with 8-μm pores in 1 ml of basal medium and 250 μl on the top of the transwell. Cells were then stimulated by vehicle, rhNAMPT (20 μg/ml) with or without FK866 (10 μM) for 48 hrs. Unmigrated cells were then scraped from the top of the filter and the migrated bottom layer of cells were stained by 1% aqueous Crystal Violet solution (Electron Microscopy Sciences, Cat.# RT 26088-10). The transwell bottom was gently separated by a blade and put on a glass slide for imaging. The migrated cells were counted and quantified. Images were taken by an Olympus BX51 Fluorescence Microscope and processed by DPController Software (Oylmpus IMS). C) In wound healing assays, approximately 0.5 million hPASMCs were seeded to 6-well cell culture plates, a straight line was scratched using a 200-μl pipette tip after cells

reached 100% confluence. Three red dots were labelled beside each line. The cells were immediately washed by culture medium and then starved with M199 medium including 0.1% FBS for 3 hours, followed by stimulation with vehicle or rhNAMPT (20 μg/ml) with or without FK866 (10 μM). The cells were imaged at 6 hrs after stimulation. Image J software was used to measure the wound line width for all the three spots labeled in each line. Wound closure% = {[width (start point)-width (end point)] /width (start point)} x 100% was calculated (ANOVA $P < 0.05$). Size bar: 50 μm. $^{**}P < 0.01$.

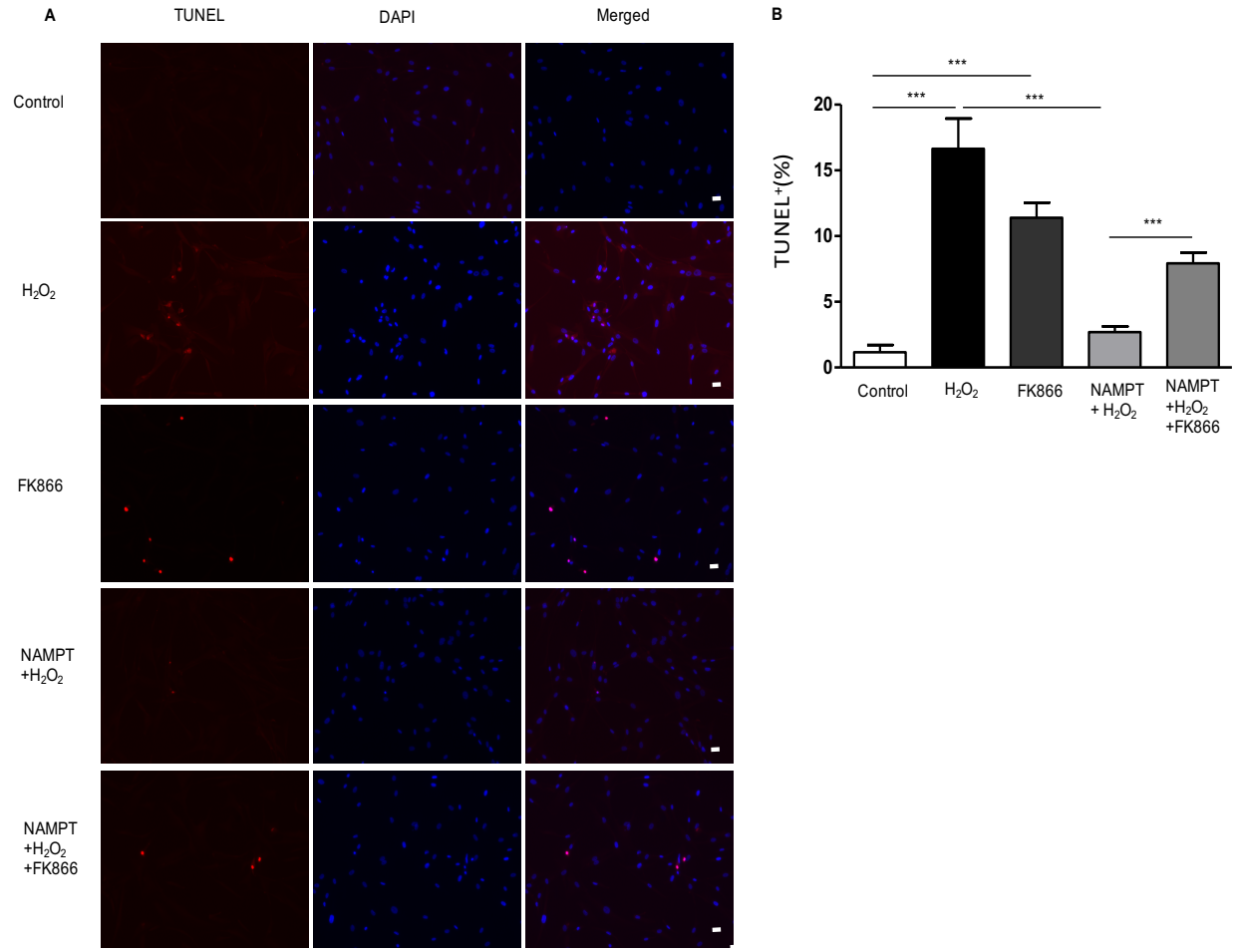

Figure S10. TUNEL assays reveal that rhNAMPT protein inhibits hPASMC apoptosis and FK866 protmotes cell apoptosis. A) Representative images and B) quantitative data from TUNEL assays. hPASMCs were cultured on a coverslip in a 6-well cell culture plate. H_2O_2 (100μM, Sigma, Cat.# ab66110) was used as an apoptosis stimulus for hPASMCs. When cell confluence reached 95%, cells were starved for 3 hrs and stimulated by H_2O_2, FK866 (10 μM), H_2O_2 + rhNAMPT (20 μg/ml) or H_2O_2 + rhNAMPT (20 μg/ml) with FK866 (10 μM) for 24 hrs. Cell apoptosis was examined using an *in situ* BrdU–Red DNA fragmentation (TUNEL) kit. The cells on the coverslips were examined using a Nikon Eclipse E800 fluorescence microscope, and the images were processed by MetaMorph software (Molecular Devices, Inc.). Approximately ten images were taken from each condition, and over 500 cells were counted according to DAPI staining. Representative images from each group were demonstrated. Size bar: 50 μm. Number of TUNEL positive cells was quantified and shown in panel B. ***$P < 0.001$.

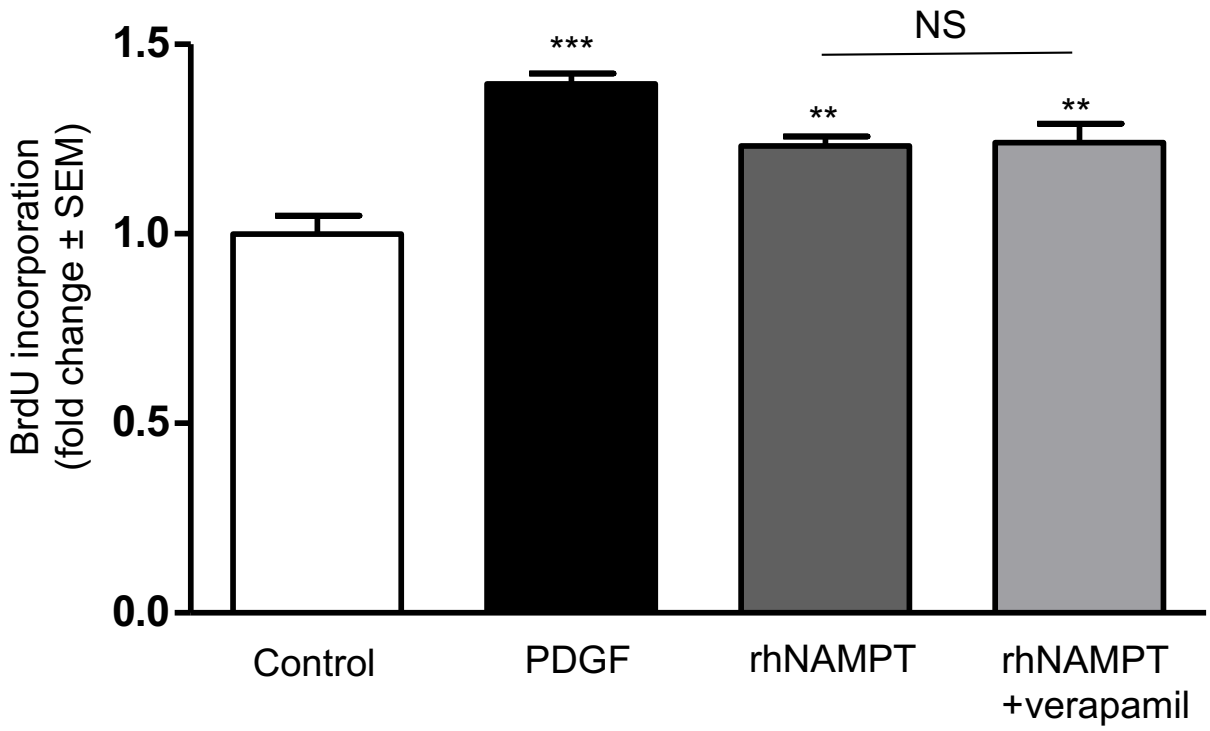

Figure S11. Blockage of L-type channels with verapamil does not affect rhNAMPT mediated hPASMC proliferation. hPASMCs were treated with verapamil (10 μM) for 48 hours, rhNAMPT (20 μg/ml) was used to stimulate hPASMC proliferation via BrdU incorporation assays. PDGF (20 ng/ml) was used a positive control. Results are expressed as mean ± SEM; n = 6 per group. $^{**}P < 0.01$; $^{***}P < 0.001$ vs control.

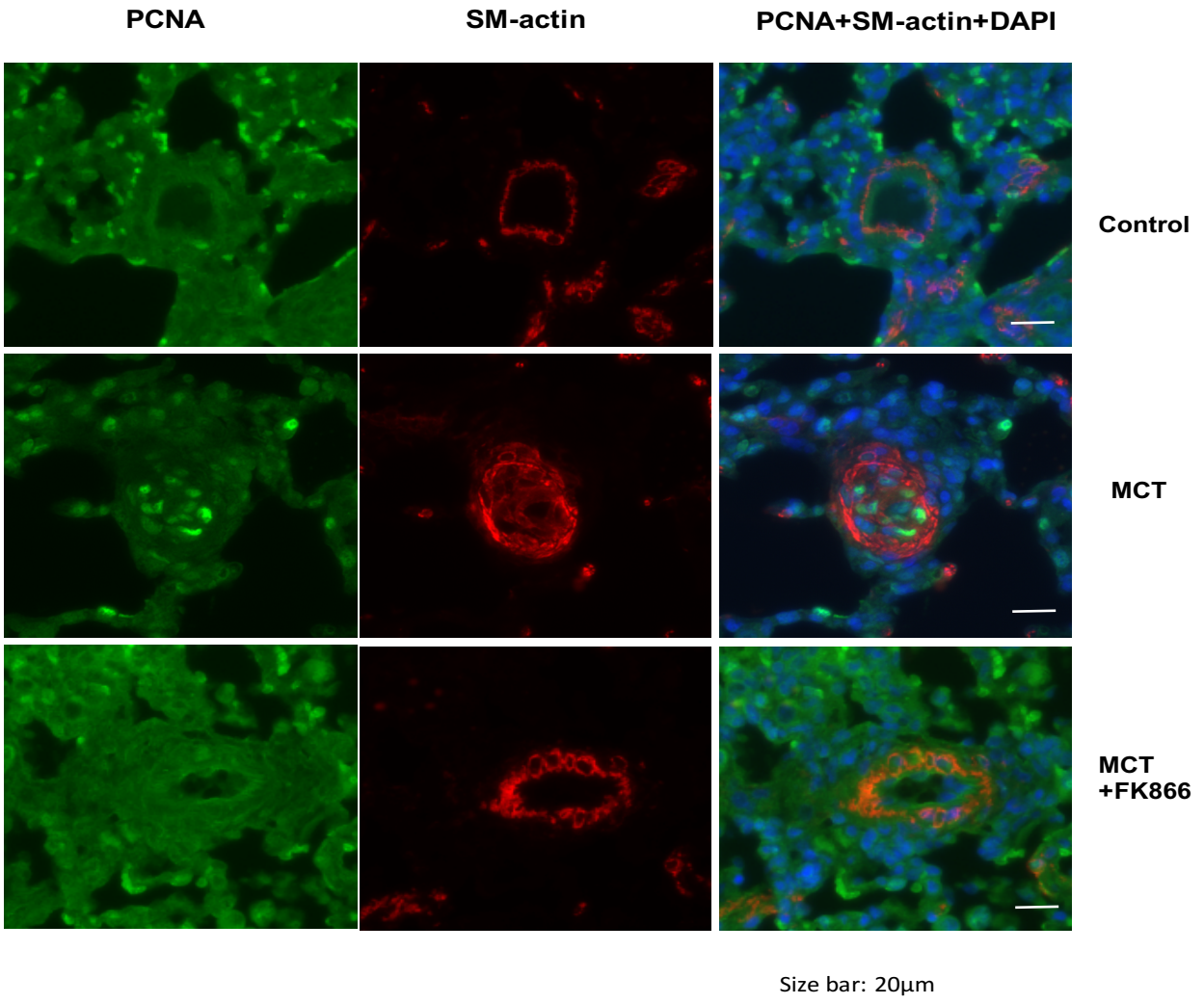

Figure S12. NAMPT inhibition decreases PASMC proliferation in MCT-mediated PH. PASMCs from FK866 treated group in the monocrotaline-mediated rat PH model exhibit lower proliferation demonstrated by immunohistochemistry. The procedure is similar to human lung immunofluorescence staining. PASMCs were stained with Cy3™ labeled anti-α-smooth muscle actin antibodies (1:300) and proliferating cells were examined by rabbit anti-PCNA antibodies (1:100) followed by Alexa Fluor® 488 Donkey anti-Rabbit IgG antibody (1:500) staining. Representative pulmonary artery images demonstrate that, when compared to WT controls, SphK1-/- mice exhibited decreased medial hypertrophy, which was associated with a decreased number of proliferating PASMCs in response to chronic hypoxia. PASMC positive cells are depicted in red, and proliferating PCNA positive nuclei are green. Size bar: 20 μm.

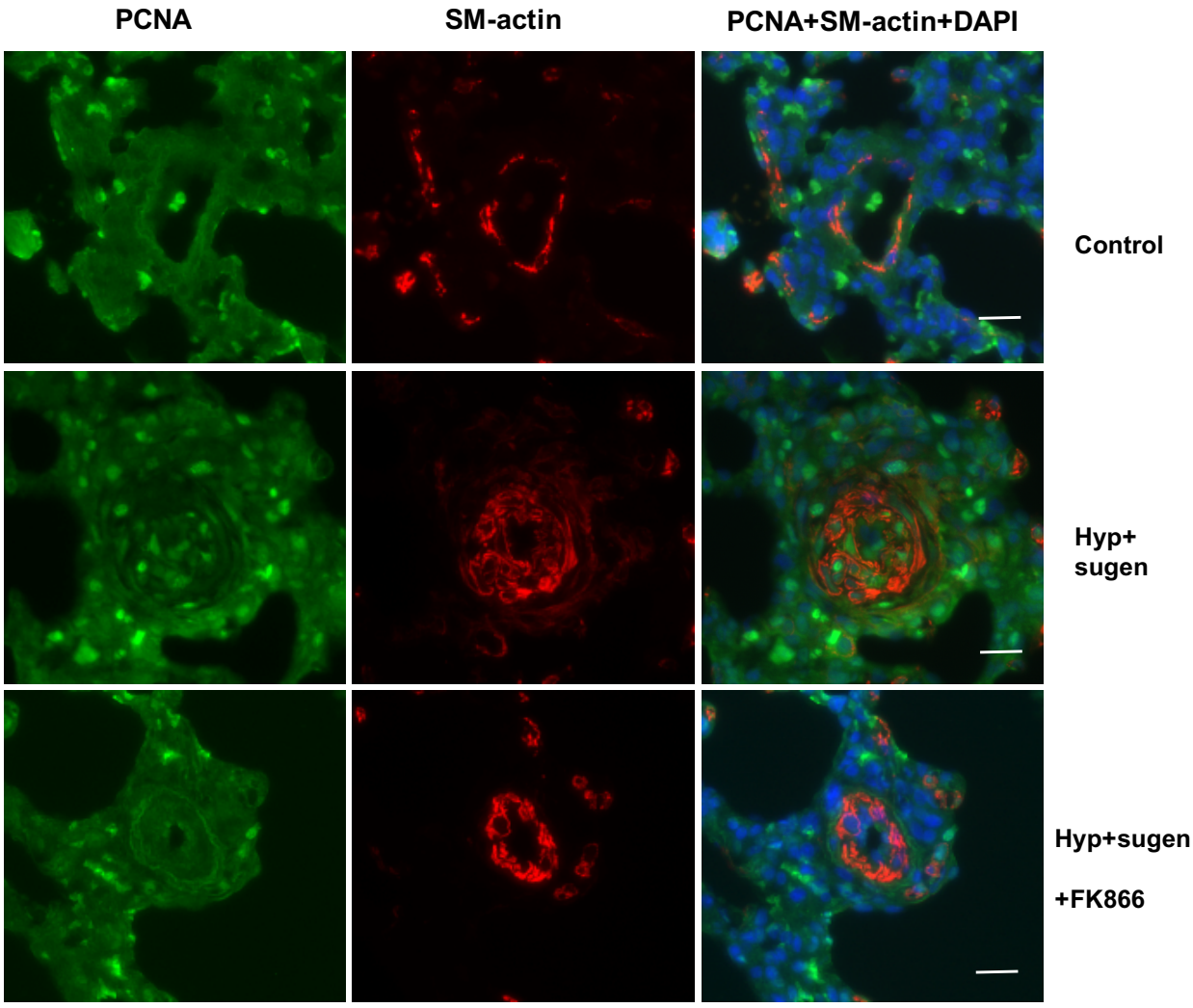

Figure S13. NAMPT inhibition decreases PASMC proliferation in Sugen-hypoxia mediated PH. PASMCs from FK866 treated group in the hypoxia plus sugen-mediated rat PH model exhibit lower proliferation demonstrated by immunohistochemistry. The procedure is mentioned in Figure S12. Size bar: 20 μm.

Supplemental References:

1. Chen J, Tang H, Sysol JR, Moreno-Vinasco L, Shioura KM, Chen T, Gorshkova I, Wang L, Huang LS, Usatyuk PV, Sammani S, Zhou G, Raj JU, Garcia JG, Berdyshev E, Yuan JX, Natarajan V and Machado RF. The sphingosine kinase 1/sphingosine-1-phosphate pathway in pulmonary arterial hypertension. *Am J Respir Crit Care Med*. 2014;190:1032-43.
2. Zeineh NS, Bachman TN, El-Haddad H and Champion HC. Effects of acute intravenous iloprost on right ventricular hemodynamics in rats with chronic pulmonary hypertension. *Pulm Circ*. 2014;4:612-8.